

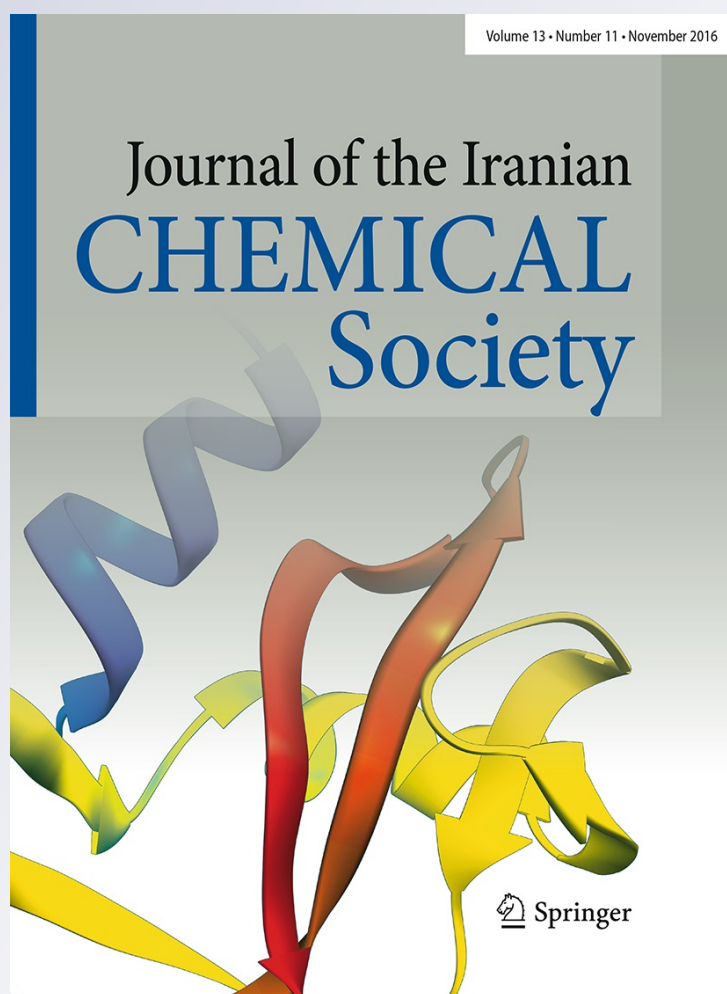
Synthesis and characterization of chitosan coating of NiFe₂O₄ nanoparticles for biomedical applications

Saeid Ramezani, Arash Ghazitabar & Seyed Khatiboleslam Sadrnezhaad

Journal of the Iranian Chemical Society

ISSN 1735-207X
Volume 13
Number 11

J IRAN CHEM SOC (2016) 13:2069-2076
DOI 10.1007/s13738-016-0924-9



Your article is protected by copyright and all rights are held exclusively by Iranian Chemical Society. This e-offprint is for personal use only and shall not be self-archived in electronic repositories. If you wish to self-archive your article, please use the accepted manuscript version for posting on your own website. You may further deposit the accepted manuscript version in any repository, provided it is only made publicly available 12 months after official publication or later and provided acknowledgement is given to the original source of publication and a link is inserted to the published article on Springer's website. The link must be accompanied by the following text: "The final publication is available at link.springer.com".

Synthesis and characterization of chitosan coating of NiFe₂O₄ nanoparticles for biomedical applications

Saeid Ramezani¹ · Arash Ghazitabar²  · Sayed Khatiboleslam Sadrnezhaad³

Received: 24 January 2016 / Accepted: 21 June 2016 / Published online: 27 June 2016
© Iranian Chemical Society 2016

Abstract Nickel ferrite nanoparticle is a soft magnetic material whose appealing properties as well as various technical applications have rendered it as one of the most attractive class of materials; its technical applications range from its utility as a sensor and catalyst to its utility in biomedical processes. The present paper focuses first on the synthesis of NiFe₂O₄ nanoparticles through co-precipitation method resulting in calcined nanoparticles that were achieved at different times and at a constant temperature (773 k). Afterward, they were dispersed in water that was mixed by chitosan. Chitosan was bonded on the surface of nanoparticles by controlling the pH of media. In order to assess the structural and magnetic properties of nanoparticles, X-ray diffraction (XRD), Fourier transform infrared spectroscopy (FTIR), transmission electron microscopy (TEM), and vibrating sample magnetometer (VSM) analyses were conducted at room temperature. As per the results of XRD analysis, the pure NiFe₂O₄ was synthesized. Additionally, nanoparticles grew in size by extending the calcination process duration. TEM micrographs were used to determine the size and shape of particle;

the obtained results indicate that the particle size was in a range of 17–30 nm and of a circular shape. The proper chitosan covering was also indicated by FTIR results. The VSM analysis also revealed that the saturated magnetization of NiFe₂O₄ nanoparticles stood in a range of 29 emu/g and 45 Q_c. A stable maximum temperature ranging from 30 to 42 was successfully achieved within 10 min. Also, a specific absorption rate of up to 8.4 W/g was achieved. The study results revealed that the SAR parameter of the coated nickel ferrite nanoparticle is more than that of pure nickel ferrite or cobalt ferrite nanoparticles.

Keywords Nickel ferrite nanoparticles · Chitosan biopolymer · Hyperthermia · SAR parameter

Introduction

The recent years have witnessed so much attention directed toward nanomagnetic materials for exhibiting such outstanding magnetic qualities [1]. Ferrite nanomaterials have been the subject of much considerable and extensive research because of their magnetic quality [2].

Nickel ferrite (NiFe₂O₄) nanoparticles are known as one of the most important nanocrystalline spinel ferrites [3]. Their utility as permanent magnets and sensors and their application in magnetic resonance imaging (MRI) enhancement, catalysis, magnetically guided drug delivery, and high density information strong technology are among the various applications of these materials [4, 5].

Magnetic nanoparticles are also employed for treating cancer. Surgery, chemotherapy, radiation therapy, and hyperthermia are among cancer treatment options. The latter, clinical hyperthermia is of three broad categories, namely (1) localized hyperthermia, (2) regional

✉ Arash Ghazitabar
Arash_Ghazitabar@aut.ac.ir

Saeid Ramezani
saeedramezani68@gmail.com

Sayed Khatiboleslam Sadrnezhaad
sadrnezh@sharif.edu

¹ Department of Biomedical Engineering, Science and Research Branch, Islamic Azad University, Tehran, Iran

² Department of Mining and Metallurgical Engineering, Amirkabir University of Technology, Tehran, Iran

³ Department of Materials Science and Engineering, Sharif University of Technology, Tehran, Iran

hyperthermia, and (3) whole-body hyperthermia. In this type of treatment, specific tissues or organs are heated (41–46 °C) for tumor/cancer therapy; the heat can be generated by radio frequency, microwave, or laser wavelengths. The physical phenomenon of losses can be used to partially obtain the desired heat. In order to achieve the favorite temperature rise enhancement with low concentration of nanoparticles, it is desirable to have a high specific loss power (SLP) heat generated per unit mass of nanoparticles. In addition to field parameters, the specific loss power of nanoparticle dispersion depends highly on particle size, size distribution, anisotropy constant, saturation magnetization, and surface modification [6, 7].

NiFe₂O₄ is of a cubic structure that is of an inverse spinel form. Fe²⁺ and Ni²⁺ ions populate tetrahedral sites in this structure [8]. As a proper method, chemical route is generally used for the preparation of the spinel nanoparticles. Nickel ferrite is one of the most significant spinel ferrites. It is of a particular ferromagnetism quality that originates from the magnetic moment of antiparallel spins [9]. Several methods can be employed for the synthesis of (NiFe₂O₄) nanoparticles; they include: heat treatment [10], co-precipitation [11], chemical methods [12], sonochemical [13], sol–gel [14], and thermal decomposition [15, 16]. Nevertheless, the strong dipole–dipole interaction causes the tendency of these NiFe₂O₄ nanoparticles to aggregate; hence, it is required to modify their surface with biocompatible and biodegradable polymers.

As per the conducted literature review, starch [17], chitosan [17, 18], polyvinyl alcohol [17, 19], polyethylene glycol (PEG) [17, 20], oleic acid [21], dextran [17, 19, 22], and lauric acid [22] are the most appealing polymeric materials for surface coating of magnetic nanoparticles.

Chitosan is a polyaminosaccharide that is of many proper biological and chemical properties. It is not an expensive biopolymer and has reactive groups (OH and NH₂) which establish significant interactions with the surface of nanoparticles [23, 24].

In the present study, an attempt has been made to prepare the NiFe₂O₄ nanoparticles through co-precipitation method that has proved to be a proper technique for making small-sized and monodisperse nanoparticles. And then, the suspension cross-linking technique was used for the preparation of chitosan coating on nanoparticles; glutaraldehyde was also used as a cross-linker. The nanoparticles were characterized by X-ray diffraction (XRD), vibrating sample magnetometer (VSM), scanning electron microscopy (SEM), and Fourier transform infrared spectroscopy (FTIR) techniques. Finally, due to the noticeable magnetic properties of NiFe₂O₄, the specific absorption rate (SAR) was calculated and compared with those in the literature.

Materials and methods

Materials

The materials used for synthesis included chloride salts (NiCl₂·6H₂O and FeCl₃·6H₂O), sodium hydroxide, aqueous acetic acid, ammonia solution, and oleic acid. All these chemicals were of analytical grade from Merck Company. Furthermore, chitosan was used for surface coating of nanoparticles obtained from Sigma-Aldrich. PBS pellets were purchased from China Company. All the glassware was cleaned by aqua regia (v/v, HCl/HNO₃, 3:1)¹ and thoroughly rinsed with deionized water prior to commencement of experiments.

The employed XRD system was the Xpert Philips model made in Netherlands. The source of X-ray was Cu Kα with a wavelength of 1.54 Å. The step of scanning was 0.02° with the speed of one step per second. The TEM system used for morphology and size determination was JEOL JEM-2100 FTEM model. The SEM system used for morphology of sample was CAMSCAN MV2300 model with 15 kV applied voltage. Fourier transform infrared spectroscopy (FTIR) spectra were obtained using a Tensor 27 FTIR spectrometer (Bruker), and samples were dried at 50 °C. Vibration sample magnetometer (VSM) measurements were made on a Lakeshore model 7300 VSM system.

Synthesis of NiFe₂O₄ nanoparticles

Firstly, 0.2 M NiCl₂·6H₂O and 0.4 M FeCl₃·6H₂O solutions were prepared separately. The solutions were then mixed with one another, and sodium hydroxide solution (3 M) was added drop-wise to the final solution till pH was adjusted to around 13.

Oleic acid was added to the solution as a surfactant. And then, the temperature was increased up to 80 °C for 40 min. Finally, the solution was centrifuged and washed with water and ethanol several times. The precipitation was dried in an oven at 80 °C for several hours. Amorphous NiFe₂O₄ nanoparticles were obtained at this stage, and an additional process was used for obtaining the crystalline powder of nickel ferrite nanoparticles [25–27].

Chitosan coating process

Chitosan solutions of 0.5 wt% were prepared by dissolving the required amount of chitosan powder in 40 mL of a 2 % acetic acid solution. Ten milliliters of the solution containing synthesized NiFe₂O₄ nanoparticles was blended

¹ Caution: aqua regia is an extremely toxic chemical and should be handled with care!

with the prepared 0.5 wt% chitosan solution with vigorous stirring. Five milliliters of a 25 % NH_4OH solution was then added to the mixture. After the reaction, the chitosan-coated nickel ferrite was washed with water, resuspended in 20 mL of a 0.5 % acetic acid solution, and dispersed in a PBS solution by ultrasonication for 20 min [28].

Results and discussion

Particle size and structure of chitosan coating of NiFe_2O_4 nanoparticles

Figure 1 shows the morphology of both pure NiFe_2O_4 and NiFe_2O_4 -chitosan nanoparticles. The nanoscaled nickel ferrite particles were of a small size before and after

coating by chitosan. As shown in Fig. 1, NiFe_2O_4 particles were approximately monodisperse with a mean diameter of 17–20 nm. Based on the TEM micrographs, it is clear that the obtained nanoparticles are uniform and in the shape of spheres. The TEM image of NiFe_2O_4 -chitosan nanoparticles (Fig. 2b) shows that the structure of chitosan-coated NiFe_2O_4 nanoparticles was better, causing the enhancement of the surface; the average diameter of such a structure was 23–30 nm. The average size of grain obtained from TEM image of samples is in good agreement with the size determined by Scherer equation from XRD patterns.

Figure 2a, b shows the surface morphology of pure NiFe_2O_4 nanoparticles and chitosan-coated NiFe_2O_4 nanoparticles. It can be observed in SEM and FESEM images that uncoated NiFe_2O_4 nanoparticles are highly agglomerated, while chitosan-coated NiFe_2O_4 nanoparticles

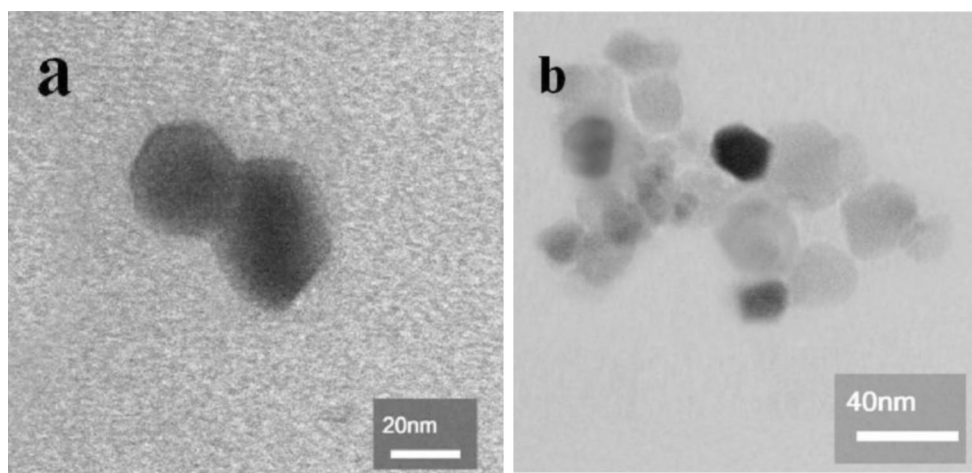


Fig. 1 TEM image of pure NiFe_2O_4 nanoparticles (a) and NiFe_2O_4 -chitosan nanoparticles (b)

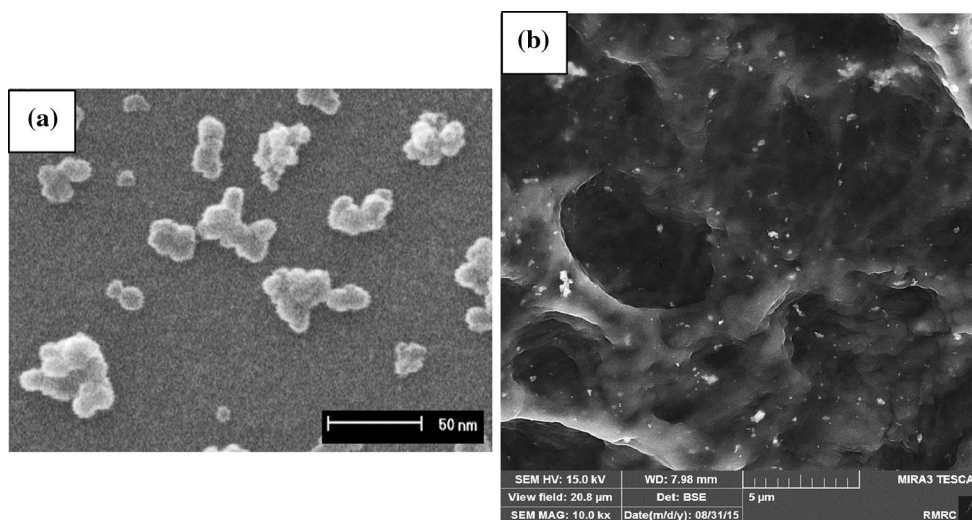


Fig. 2 SEM image of pure NiFe_2O_4 nanoparticles (a) and FESEM image of NiFe_2O_4 -chitosan nanoparticles (b)

enjoy well-dispersed structures in the polymeric shell of chitosan. This may be due to the coating of chitosan on nanoparticles.

Phase structure of NiFe₂O₄ nanoparticles

The XRD patterns of calcined NiFe₂O₄ samples are shown in Fig. 3a–c. In this figure, the patterns introduced three time intervals of 1, 2, and 3 h for calcination process at the constant temperature.

All of the patterns show that the peaks correspond to the planes (3 1 1), (4 4 0), (2 2 0), confirming the phase formation of NiFe₂O₄ with a well-defined spinel structure. However, no impurities are observed in Fig. 3b which belongs to the calcination process conducted for 2 h at the same temperature [29, 30].

In the patterns of XRD diffraction, the broad nature of the diffraction bands indicated that NiFe₂O₄ had small particle sizes [30]. The particle sizes can also be quantitatively evaluated from the XRD data using Debye–Scherrer equation which yields the equation for the relationship between peak broadening in XRD and particle size [31]:

$$d = (k\lambda/\beta \cos \theta)$$

According to Debye–Scherrer equation (2), the size of NiFe₂O₄ nanoparticles is about 15, 18, and 24 nm for 1, 2, and 3 h of calcination, respectively. The values of the lattice parameter were about 0.911 nm that were reported for NiFe₂O₄ ($a = 0.8339$ nm) in the standard data (JCPDS: 10-0325).

The sample that was calcined for 2 h was selected for chitosan coating process for its proper crystallinity.

FTIR spectra analysis

Figure 4 shows FTIR spectra of pure NiFe₂O₄ nanoparticles (a) and NiFe₂O₄–chitosan nanoparticles (b) that were recorded between 400 and 4000 cm⁻¹.

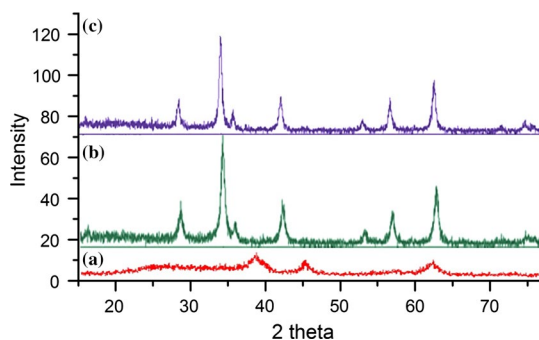


Fig. 3 X-ray diffraction of pure NiFe₂O₄ nanoparticles after 1 h of calcination (a), 2 h of calcination (b) and 3 h of calcination (c)

Figure 4a shows that two absorption bands around 589 and 424 cm⁻¹ are attributed to tetrahedral and octahedral complexes, respectively [32].

The peaks at 589 cm⁻¹ relate to Fe–O bond that are shown at 600 cm⁻¹ after chitosan coating (b). As shown in Fig. 4b, the peak around 3390 cm⁻¹ indicates the OH group. In Fig. 4b, the characteristic absorption bands appeared at 1520 cm⁻¹ which can be assigned to N–H bending vibration; peaks of 1300 cm⁻¹ appeared in C–O stretching alcoholic group in chitosan. The new sharp peak of 1626 cm⁻¹ appeared indicating that chitosan reacted with glutaraldehyde to form the Schiff base. The emergence of Fe–O bond can be attributed to the new sharp peak 600 cm⁻¹. In Fig. 4b, the characteristic bond of CH₂ group, as present in chitosan, is represented by a band at about 2900 cm⁻¹ [26, 33, 38].

The obtained results showed that NiFe₂O₄ nanoparticles were successfully coated by chitosan. As the negatively charged surface of nickel ferrite has an affinity with chitosan, it can coat the NiFe₂O₄ nanoparticles by electrostatic interaction and chemical reaction through glutaraldehyde cross-linking.

Thermo-gravimetric analysis

Thermo-gravimetric analyzer from AT instruments was employed for thermo-gravimetric analysis (TGA) of ferrofluids in a dry state at a heating rate of 101 °C/min under nitrogen atmosphere. Figure 5 shows the recorded weight loss of representative samples that occurred as a result of temperature increase. The TG curve in Fig. 5 indicates a dramatic weight loss step from 0 °C up to about 100 °C,

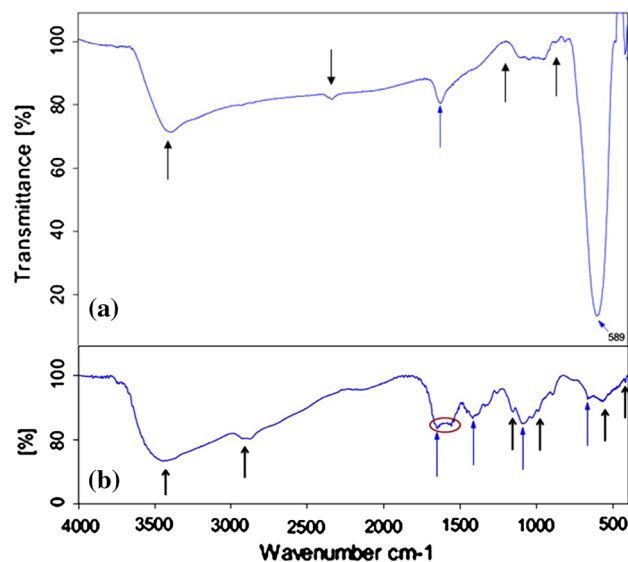
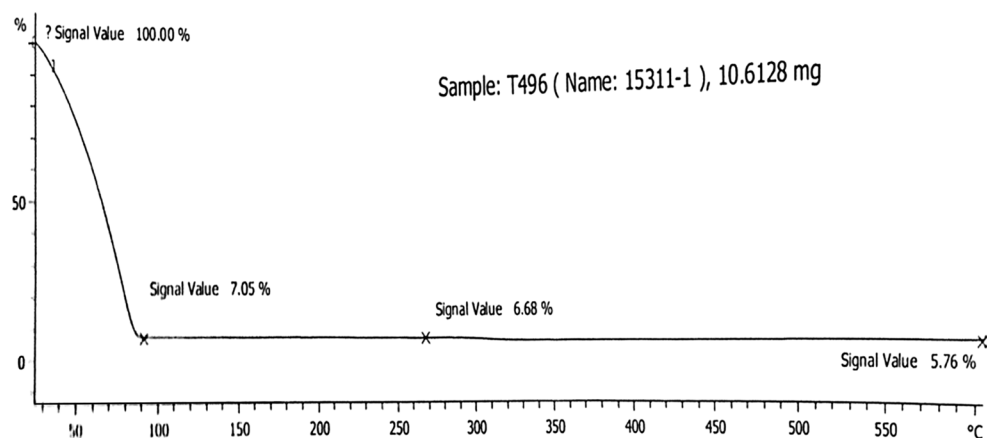


Fig. 4 FTIR spectra of pure NiFe₂O₄ nanoparticles after 2 h of calcination (a) and NiFe₂O₄–chitosan nanoparticles (b)

Fig. 5 Thermogravimetric of NiFe₂O₄ nanoparticles after 2 h of calcinations and coated with chitosan



with a further slight weight loss observed until 300 °C. The loss of moisture and trapped solvent (water and carbon dioxide) accounted for the major weight loss, while the combustion of coated chitosan accounted for the minor weight loss. The formation of nanocrystalline NiFe₂O₄ as the decomposition product is indicated by the plateau formed between 300 and 600 °C on the TG curve; this is confirmed by XRD and FTIR analysis, as illustrated in Figs. 3 and 4, respectively.

Magnetic properties of nanoparticles

The magnetic quality of NiFe₂O₄ with an inverse spinel structure can be explained in terms of the distribution of cations and the magnetization that is caused by Fe³⁺ ions at both tetrahedral and octahedral sites as well as Ni²⁺ ions at octahedral sites.

Figure 6 illustrates the particular magnetization curves of the precursor and calcined NiFe₂O₄ nanoparticles that were obtained at room temperature.

Hysteresis loops can typically be found in soft magnetic materials; these loops indicate hysteresis ferromagnetism in the field range of $\sim\pm 10,000$ Oe; specific saturation magnetization (M_s) values of 4, 29.5, and 28.5 emu/g were observed for NiFe₂O₄ sample calcined at 823 K for 60, 120, and 180 min, respectively, that were lower than the bulk of NiFe₂O₄ (50 emu/g) [34]. It was also observed that the tendency of M_s to increase is consistent with the enhancement of crystallinity from 60 to 120 min; also the values of M_s decrease from 120 to 180 min due to the increase in particle size. It is commonly known that the size affects the magnetic quality of magnetic particles dramatically. Each of the magnetic nanoparticles is usually of a single magnetic domain. For relatively larger particles, the static magnetic energy is usually reduced by magnetic domains that are formed [33]. A decrease in particle size results in a decrease in the number of domains. The particles turn into single domain particles of a size under a

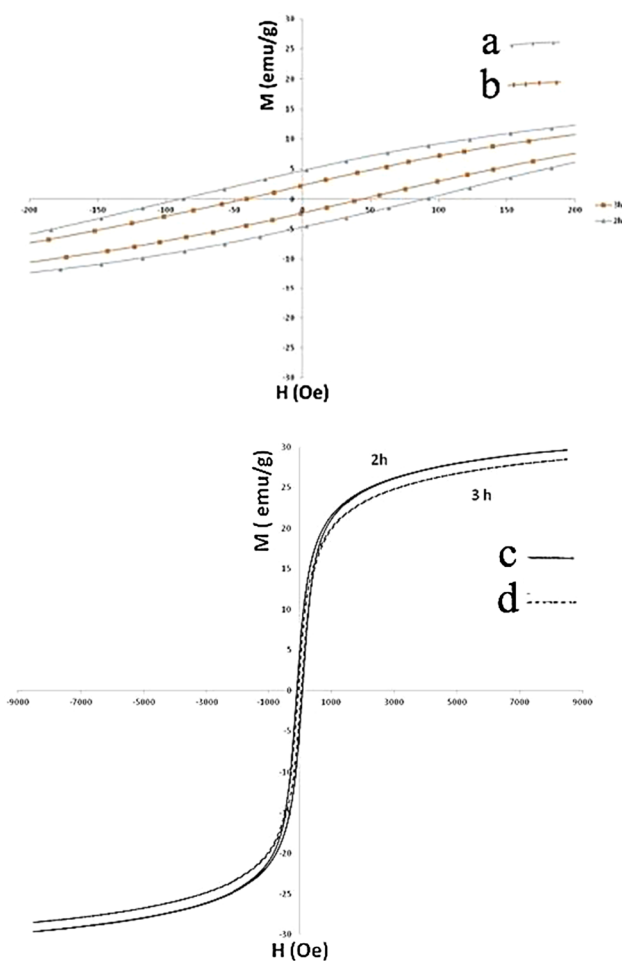


Fig. 6 Magnetic properties of NiFe₂O₄—2 h of calcinations (a), NiFe₂O₄—3 h of calcinations (b), NiFe₂O₄—2 h of calcinations (wide range) (c), NiFe₂O₄—3 h of calcinations (wide range) (d)

critical radius (for nickel ferrite, this parameter is about 100 nm) [35].

The increasing and decreasing field sides (blanket) yielded a coercive force (H_c) of 90 (–95) and 45 (–40) Oe for the

Fig. 7 Changes in specific saturation magnetization with the degree of calcination time (a) and changes in coercivity with the degree of calcination time (b)

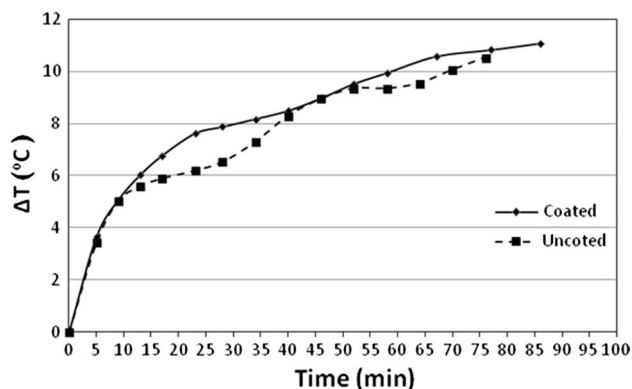
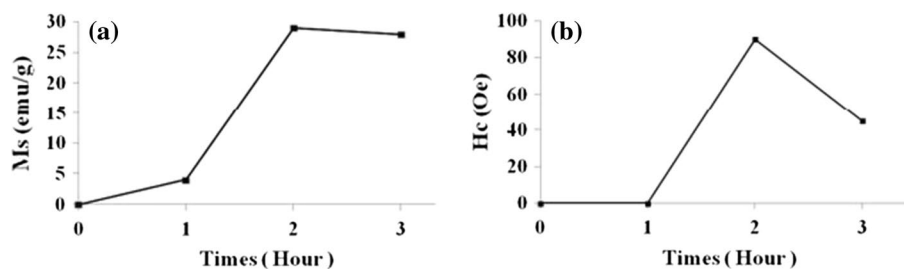


Fig. 8 Temperature increase in pure NiFe₂O₄ nanoparticles after 2 h of calcination and NiFe₂O₄-chitosan nanoparticles as a function of time

NiFe₂O₄ samples calcined for 120 and 180 min, respectively. It can be observed as per these results that an increase in particle size leads to a drop in the value of coercivity. The domain structure, critical diameter, and anisotropy of crystal can account for such variation of H_c with particle size. Should it be of a single domain, a crystallite will spontaneously break up into several domains so as to decrease the large magnetization energy it would have [19, 35].

Hyperthermia

Figure 7 illustrates that, in comparison with other nanoparticles, NiFe₂O₄ nanoparticles (calcined for 120 min) are of higher magnetization and greater magnetic heating loss.

Offering a moderate magnetic moment, chemical stability, and a high specific absorption rate (SAR) makes nanoferrites good candidates for hyperthermic purposes [19]. The SAR was measured at room temperature using the heating yielded experimentally by the nanoparticles that calcined for 120 min (Fig. 8).

As shown in Table 1, NiFe₂O₄ chitosan-coated nanoparticles, compared with those in the previous studies, were of a reasonably high SAR at the physiologically expected frequency around 300 kHz [36].

The attained SAR stood at about 3.5 and 6 for cobalt ferrite at the same conditions [37]. A remarkably small SAR

Table 1 SAR of pure NiFe₂O₄ nanoparticles after 2 h of calcination and NiFe₂O₄-chitosan nanoparticles

Sample	SAR (W/g)	
	Uncoated	With coating
Calcined NiFe ₂ O ₄	2.17	8.47

was exhibited by uncoated NiFe₂O₄ nanoparticles, even at the same frequency. As shown in Fig. 7, the temperature rose by an increase in time. The principal purpose of hyperthermic applications is generating a higher value of magnetic heat by a stable fluid in a lower exposure time. Ni ferrite is of the highest level of SAR parameter in comparison with the other mentioned ferrites in biological applications (5 kA/m, 300 kHz).

Thus, NiFe₂O₄ nanoparticles, for their high SAR at the physiologically tolerable range of applied magnetic fields and frequencies, can be a potential candidate as a clinical hyperthermic agent.

Conclusion

Synthesis through co-precipitation was favorable for obtaining crystalline powders with nanosized nickel ferrite particles. The XRD measurements and TEM images confirmed that nanoparticles were dispersed uniformly (monodispersed) and were sphere in shape with a mean diameter of about 17–30 nm, respectively.

The results obtained from FTIR and SEM indicate that NiFe₂O₄ nanoparticles were effectively coated by chitosan for various biomedical applications.

Calcined samples show that the size of particles increases by a rise in calcination temperature. High-temperature calcinations also lead to an increase in the crystallinity of samples. It was verified that ferromagnetic NiFe₂O₄ nanoparticles were coated and were of proper magnetic and structural properties; they were also of a high SAR for a hyperthermic agent application. Particularly, the adequately high heating temperature of the solid-state NiFe₂O₄ nanoparticles were readily controlled in the range of 30–45 °C at the physiologically tolerable and biological safe range of

the applied magnetic field; this allowed NiFe₂O₄ nanoparticles to be considered as a promising potential candidate as an in vivo hyperthermic agent.

Acknowledgments I would like to take this opportunity to express my deepest gratitude for the support that I have received during these past years. Special thanks to Nano System Pars Co (NATSYCO) for manufacturing the device (hyperthermia test) that is crucial in this work.

References

1. S. Mostaghim, M. Naderi, A. Ghazitabar, Synthesis of magnetite–gold nanoshells by means of the secondary gold resource. *J. Iran. Chem. Soc.* **12**, 1709–1716 (2015)
2. R. Ranjbar, M. Naderi, H. Omidvar, G. Amoabedini, Gold recovery from copper anode slime by means of magnetite nanoparticles (MNPs). *Hydrometallurgy* **143**, 54–59 (2014)
3. H. Nathani, S. Gubbala, R.D.K. Misra, Magnetic behavior of nanocrystalline nickel ferrite: part I. The effect of surface roughness. *J. Mater. Sci. Eng. B* **121**(1–2), 126–136 (2005)
4. M. Sugimoto, The past, present, and future of ferrites. *J. Am. Ceram. Soc.* **82**(2), 269 (1999)
5. Y.L. Liu, Z.M. Liu, Y. Yang, H.F. Yang, G.L. Shen, R.Q. Yu, Simple synthesis of MgFe₂O₄ nanoparticles as gas sensing materials. *Sens. Actuators B* **107**, 600–604 (2005)
6. J. Giri, P. Pradhan, T. Sriharsha, D. Bahadur, Preparation and investigation of potentiality of different soft ferrites for hyperthermia applications. *J. Appl. Phys.* **97**, 913 (2005)
7. S. Dutz, J.H. Clement, D. Eberbeck, T. Gelbrich, R. Hergt, R. Muller, J. Wotschadlo, M. Zeisberger, Ferro fluids of magnetic multicore nanoparticles for biomedical applications. *J. Magn. Magn. Mater.* **321**, 1501–1504 (2009)
8. T. Giannakopoulou, L. Kompotiatis, A. Kontogeorgakos, G. Kordas, Microwave behavior of ferrites prepared via sol–gel method. *J. Magn. Magn. Mater.* **246**(3), 360–365 (2002)
9. S. Son, M. Taheri, E. Carpenter, V.G. Harris, M.E. McHenry, Synthesis of ferrite and nickel ferrite nanoparticles using radio-frequency thermal plasma torch. *J. Appl. Phys.* **91**(10), 7589 (2002)
10. M. Salavati-Niasari, F. Davar, Z. Fereshteh, Synthesis of nickel and nickel oxide nanoparticles via heat-treatment of simple octanoate precursor. *J. Alloys Compd.* **494**, 410–414 (2010)
11. M. Salavati-Niasari, F. Davar, T. Mahmoudi, A simple route to synthesize nanocrystalline nickel ferrite (NiFe₂O₄) in the presence of octanoic acid as a surfactant. *J. Polyhedron.* **28**, 1455–1458 (2009)
12. J. Saffari, H. Shams, D. Ghanbari, A. Esmaeili, A simple chemical method for synthesis of NiFe₂O₄ nanoparticles and polystyrene-based magnetic nanocomposites. *J. Clust. Sci.* **25**, 1225–1236 (2014)
13. J. Lai, K.V.P.M. Shafi, A. Ulman, K. Loos, N.L. Yang, M.H. Cui, T. Vogt, C. Estournes, D.C. Locke, Mixed iron–manganese oxide nanoparticles. *J. Phys. Chem. B* **108**, 14876–14883 (2004)
14. F. Ansaria, A. Sobhanib, M. Salavati-Niasaria, Facile synthesis, characterization and magnetic property of CuFe₁₂O₁₉ nanostructures via a sol–gel auto-combustion process. *J. Magn. Magn. Mater.* **401**, 362–369 (2016)
15. M. Salavati-Niasari, F. Davar, M. Mazaheri, M. Shaterian, Preparation of cobalt nanoparticles from [bis(salicylidene)cobalt(II)]–oleylamine complex by thermal decomposition. *J. Magn. Magn. Mater.* **320**, 575–578 (2008)
16. M. Salavati-Niasari, N. Noshin, F. Davar, Synthesis and characterization of NiO nanoclusters via thermal decomposition. *J. Polyhedron.* **28**, 1111–1114 (2009)
17. M. Mahmoudi, S. Sant, B. Wang, S. Laurent, T. Sen, Superparamagnetic iron oxide nanoparticles (SPIONs): development, surface modification and applications in chemotherapy. *Adv. Drug Deliv. Rev.* **63**, 24–26 (2011)
18. D.T.K. Dung, T.H. Hai, L.H. Phuc, B.D. Long, L.K. Vinh, P.N. Truc, Preparation and characterization of magnetic nanoparticles with chitosan coating. *J. Phys. Conf. Ser.* **187**, 012036 (2009)
19. A.K. Gupta, M. Gupta, Synthesis and surface engineering of iron oxide nanoparticles for biomedical applications. *Biomaterials* **26**, 3995–4021 (2005)
20. A. Thangaraja, V. Savitha, K. Jegatheesan, Preparation and characterization of polyethylene glycol coated silica nanoparticles for drug delivery application. *Int. J. Nanotechnol. Appl.* **1**, 31–38 (2010)
21. L. Zhang, R. He, Oleic acid coating on the monodisperse magnetite nanoparticles. *Appl. Surf. Sci.* **253**, 2611–2617 (2006)
22. P. Pradhan, J. Giri, R. Banerjee, J. Bellare, D. Bahadur, Cellular interactions of lauric acid and dextran-coated magnetite nanoparticles. *J. Magn. Magn. Mater.* **311**, 282–287 (2007)
23. W. Weecharangsan, P. Opanasopit, T. Ngawhirunpa, A. Apirakamwong, T. Rojanarata, U. Ruktanoncha, R.J. Lee, Evaluation of chitosan salts as non-viral gene vectors in CHO-K1 cells. *Int. J. Pharm.* **161**, 348 (2008)
24. D.G. Kim, Y.I. Jeong, C. Choi, S.H. Roh, S.K. Kang, M.K. Jang, J.W. Nah, Retinol-encapsulated low molecular water-soluble chitosan nanoparticles. *Int. J. Pharm.* **319**, 130 (2006)
25. M. Aliahmad, M. Noori, N. Hatefi Kargan, M. Sargazi, Synthesis of nickel ferrite nanoparticles by co-precipitation chemical method. *Int. J. Phys. Sci.* **8**(18), 854–858 (2013)
26. B. Jacob, A. Kumar, R.P. Pant, S. Singh, E.M. Mohammed, Influence of preparation method on structural and magnetic properties of nickel ferrite nanoparticles. *Bull. Mater. Sci.* **34**(7), 1345–1350 (2011)
27. S. Imani, A.M. Zand, M. Saadati, H. Honnari, B. Maddah, Synthetics of NiFe₂O₄ nanoparticles for recombinant His-tag protein purification. *Int. J. Nano Dimens.* **2**(2), 129–135 (2011)
28. D.H. Kim, K.N. Kim, K.M. Kim, Y.K. Lee, Targeting to carcinoma cells with chitosan-and starch-coated magnetic nanoparticles for magnetic hyperthermia. *J. Biomed. Mater. Res. A* **88**(1), 1–11 (2009)
29. J. Jiang, Y.M. Yang, Facile synthesis of nanocrystalline spinel NiFe₂O₄ via a novel soft chemistry route. *Mater. Lett.* **61**, 4276–4279 (2007)
30. H. Kavas, N. Kasapoglu, A. Baykal, Y. Kaseoglu, Characterization of NiFe₂O₄ nanoparticles synthesized by various methods. *Chem. Pap.* **63**(4), 450–455 (2009)
31. B.D. Cullity, S.R. Stock, *Elements of X-ray diffraction*, 3rd edn. (Prentice-Hall, Englewood Cliffs, NJ, 2001), p. 170
32. M. Salavati-Niasari, F. Davar, T. Mahmoudi, A simple route to synthesize nanocrystalline nickel ferrite (NiFe₂O₄) in the presence of octanoic acid as a surfactant. *Polyhedron* **28**(8), 1455–1458 (2009)
33. S. Maensiri, C. Masingboon, B. Boonchomb, S. Seraphin, A simple route to synthesize nickel ferrite (NiFe₂O₄) nanoparticles using egg white. *Scr. Mater.* **56**, 797–800 (2007)
34. F. Davar, Z. Fereshteh, M. Salavati-Niasari, Nanoparticles Ni and NiO: synthesis, characterization and magnetic properties. *J. Alloys Compd.* **476**, 797–801 (2009)
35. W.C. Kim, S.L. Park, S.J. Kim, S.W. Lee, C.S. Kim, Magnetic and structural properties of ultrafine Ni–Zn–Cu ferrite grown by a sol–gel method. *J. Appl. Phys.* **87**, 6241 (2000)

36. I. Sharifi, H. Shokrollahi, S. Amiri, Ferrite-based magnetic nano-fluids used in hyperthermia applications. *J. Magn. Magn. Mater.* **324**, 903–915 (2012)
37. L.L. Lao, R.V. Ramanujan, Magnetic and hydrogel composite materials for hyperthermia applications. *J. Mater. Sci. Mater. Med.* **15**(10), 1061–1064 (2004)
38. A. Ghazitabar, M. Naderi, R. Ranjbar, A. Azadmehr, Using thio-urea ligand of gold-thiourea complex to facile direct synthesis of silica@gold core-shell nanostructures. *J. Iran. Chem. Soc.* **12**, 2253–2261 (2015)